NIH Public Access
Author Manuscript
Langmuir. Author manuscript; available in PMC 2013 July 03.

Published in final edited form as:
Langmuir. 2012 July 3; 28(26): 10082–10090. doi:10.1021/la301586t.

Tuning Smart Microgel Swelling and Responsive Behavior through Strong and Weak Polyelectrolyte Pair Assembly

Eunice Costa[1,2], **Margaret M. Lloyd**[2], **Caroline Chopko**[2], **Ana Aguiar-Ricardo**[1,*], and **Paula T. Hammond**[2,*]

[1]REQUIMTE, Departamento de Química, Faculdade de Ciências e Tecnologia, Universidade Nova de Lisboa, 2829-516 Caparica, Portugal

[2]Department of Chemical Engineering, Massachusetts Institute of Technology, Cambridge, MA 02139, USA

Abstract

The layer-by-layer (LbL) assembly of polyelectrolyte pairs on temperature and pH-sensitive cross-linked poly(*N*-isopropylacrylamide)-co-(methacrylic acid), poly(NIPAAm-co-MAA), microgels enabled a fine tuning of the gel swelling and responsive behavior according to the mobility of the assembled polyelectrolyte (PE) pair and the composition of the outermost layer. Microbeads with well-defined morphology were initially prepared by synthesis in supercritical carbon dioxide. Upon LbL assembly of polyelectrolytes, interactions between the multilayers and the soft porous microgel led to differences in swelling and thermoresponsive behavior. For the weak PE pairs, namely poly(L-lysine) / poly(L-glutamic acid) and poly(allylamine hydrochloride) / poly(acrylic acid), polycation-terminated microgels were less swollen and more thermoresponsive than native microgel; while polyanion-terminated microgels were more swollen and not significantly responsive to temperature, in a quasi-reversible process with consecutive PE assembly. For the strong PE pair, poly(diallyldimethylammonium chloride) / poly(sodium styrene sulfonate), the differences among polycation and polyanion-terminated microgels are not sustained after the first PE bilayer due to extensive ionic cross-linking between the polyelectrolytes. The tendencies across the explored systems became less noteworthy in solutions with larger ionic strength due to overall charge shielding of the polyelectrolytes and microgel. ATR FT-IR studies correlated the swelling and responsive behavior after LbL assembly on the microgels with the extent of H-bonding and alternating charge distribution within the gel. Thus, the proposed LbL strategy may be a simple and flexible way to engineer smart microgels in terms of size, surface chemistry, overall charge and permeability.

Introduction

Increasing research on the design and engineering of microparticles has enabled the preparation of highly functional materials with specific and customized properties. Initially reported for the modification of planar surfaces,[1] the layer-by-layer (LbL) assembly method has been thoroughly applied to microparticles for a diverse range of applications, such as biosensing,[2,3] controlled delivery of therapeutics,[4] optical sensing,[5] and materials encapsulation.[6] This approach is based on the consecutive adsorption of materials containing complementary charged or functional groups onto a surface, yielding nanoscaled thin

air@fct.unl.pt; hammond@mit.edu.

Supporting Information Available: Zeta potential of poly(NIPAAm-co-MAA) microgels with increasing relative amounts of MAA; optical micrographs of LbL assembled PP9010 microgels; and ATR FT-IR spectral analysis of the PP9010 copolymer and used polyelectrolytes before and after multilayer assembly. This material is available free of charge via the Internet at http://pubs.acs.org.

NIH-PA Author Manuscript
NIH-PA Author Manuscript
NIH-PA Author Manuscript

NIH-PA Author Manuscript

NIH-PA Author Manuscript

NIH-PA Author Manuscript

films.[1,7] The LbL method renders a precise control over the surface interfacial properties by varying the specific complementary materials being used, the build-up conditions and/or post-assembly modification. Extensive reports may be found on the influence of the salt concentration, ionic strength and pH on the growth and morphology of LbL multilayers to achieve different functionalities. Strong PE pairs such as poly(diallyldimethylammonium chloride) / poly(sodium styrene sulfonate) (PDAC/PSS) form thin, fully charged and highly ionically cross-linked multilayers, in which the swelling, hydrophobicity and ion transport is dependent on the presence of salts and the ionic strength.[8–11] On the other hand, for weak polyelectrolytes in which the charge density is pH-dependent, the deposition pH is a key parameter that can be systematically varied to tune the film structure, thickness and hydration, as shown for poly(allylamine hydrochloride) / poly(acrylic acid) (PAH/PAA).[8,12] This strategy has been explored to control cell adhesion,[13] film porosity,[14] or to develop nanoreactors.[15] Biologically active films with cell adhesive,[16] pro- and anticoagulant[17] or antifouling[18] properties have been prepared from synthetic polypeptides, such as poly(L-lysine) / poly(L-glutamic acid) (PLL/PGA), polysaccharides or naturally derived materials. These biocompatible films are generally more hydrated than synthetic polyelectrolytes multilayers (at comparable ionic strength) and exhibit an exponential growth regime characterized by a high mobility and interpenetration of the polymer chains.[19,20]

Smart hydrogel particles are three dimensional cross-linked polymer networks exhibiting reversible swelling responses to external stimuli, namely changes in temperature, pH and ionic strength, and have been explored for a diverse range of biotechnological applications.[21] Poly(*N*-isopropylacrylamide) (PNIPAAm) is a well-known thermosensitive polymer in which the volume phase transition occurs at a lower critical solution temperature (LCST) of about 30–32 °C.[22] The microgel collapse above the LCST is characterized by an entropy-driven destabilization of the water-amide hydrogen bonds and increasing hydrophobic interactions among isopropyl groups, leading to water expulsion.[22,23] The functionalization of PNIPAAm microgels with carboxylic acid groups via copolymerization enables pH tunability to the system, broadening their applicability. Furthermore, these groups are prone to further chemical modifications, and, when ionized, increase or suppress the LCST behavior and contribute to microgel swelling.[24] The preparation of PNIPAAm-based hydrogel particles using supercritical fluid technology offers many advantages over conventional synthesis methods, as biocompatible beads with well-defined morphology and physical properties are readily obtained without the need for extensive purification or further processing, thus making the approach especially suitable for sensitive biological applications.[25,26]

The vast majority of the literature reports regarding the LbL thin film assembly on particles concern the use of colloidal substrates as sacrificial cores for the preparation of hollow capsules.[27,28] More recently, studies concerning soft and porous beads have been developed,[2,29] in which the film morphology, the mechanism of multilayer growth and molecular conformation of the assembled polyelectrolytes is closely related to the interactions with the underlying substrate, as interpenetration of the polymer chains within the hydrogel mesh may occur. Specifically for smart carboxylic acid copolymerized PNIPAAm nanogels, it has been shown by Richtering *et al.* that the LbL assembly of polyelectrolytes modifies their physical properties and responsive behavior, depending on the location of the charges within the microgel,[30,31] the specific PE pair used,[32,33] the PE molecular weight,[31] as well as the processing conditions such as ionic strength and salt concentration.[32]

Herein, the impact of the LbL assembly of polyelectrolytes pairs with distinct intrinsic charge densities and mobility characteristics on the properties of temperature and pH-responsive poly(NIPAAm-co-MAA) micron-sized hydrogel beads synthesized in

NIH-PA Author Manuscript

NIH-PA Author Manuscript

NIH-PA Author Manuscript

supercritical carbon dioxide ($scCO_2$) is described. Furthermore, this report aims toward understanding the mechanisms of interaction between the LbL multilayers and the microgels through an FT-IR analysis approach. By examining the nature of LbL assembly on responsive microgels, it is possible to outline future directions on the use of PE multilayers to enable microgel selective permeability by tuning the mesh size, mechanical properties, and net surface charge and chemistry to achieve the desired biological activity. Indeed, the combination of the $scCO_2$ microbeads synthesis with the versatile LbL assembly technique may enable tailored microgel systems with the potential for controlled drug delivery or biomacromolecules recovery applications.

Experimental Section

Materials and Sample Preparation

N-isopropylacrylamide (NIPAAm; 97% purity), di(ethyleneglycol) dimethacrylate (DEGDMA, 95% purity), 2,2′-azobis(isobutyronitrile) (AIBN; 98% purity), methacrylic acid (MAA; 98% purity), poly(sodium styrene sulfonate) (PSS; M_w 70,000), poly(acrylic acid) (PAA; M_w 200,000, $pK_a \sim 6.5$),[12] poly(L-lysine) (PLL; M_w 30,000 – 70,000, $pK_a \sim 9$), poly(L-lysine) fluorescein isothiocyanate (PLL-FITC; 0.3–1.0 mol % of FITC per mol of monomer M_w 30,000 – 70,000), poly(L-glutamic acid) (PGA; M_w 50,000 – 70,000, $pK_a \sim 7.4$), rhodamine B isothiocyanate and anhydrous *N,N*-dimethylformamide (DMF) were purchased from Sigma-Aldrich. Krytox 157 FSL (a commercial perfluoropolyether) was purchased from DuPont. Carbon dioxide was obtained from Air Liquide with 99.998% purity. Poly(diallyldimethylammonium chloride) (PDAC; M_w 240,000; 28 wt % solution in water) and poly(allylamine hydrochloride) (PAH; M_w 120,000, $pK_a \sim 8–9$)[12] was purchased from Polysciences, Inc. Cascade blue ethylenediamine trisodium salt was purchased from Invitrogen. 1-1-ethyl-3-[3-dimethylaminopropyl]carbodiimide hydrochloride (EDC) and *N*-hydroxybenzotriazole (HOBt) were obtained from Pierce. All the materials were used without any further purification. Deionized water was purified through a Milli-Q system and had a resistivity greater than 18 MΩ.cm.

Synthesis of cross-linked poly(NIPAAm-co-MAA) microgels (90 mol % NIPAAm, 10 mol % MAA and 0.74 mol % DEGDMA relative to monomer amount), hereafter designated as PP9010 microgels, was carried out by free-radical dispersion polymerization in $scCO_2$ following an already described protocol.[26,34] Herein the monomers at a concentration of 5.2 wt % relative to CO_2 and Krytox 157 FSL at 10 wt % relative to the monomers amount were charged into a high-pressure cell at 28.0 MPa and 65 °C. At these experimental conditions, an initial homogeneous phase was obtained with all the reactants completely soluble in the supercritical medium. The reaction was allowed to proceed for 24 hours under stirring. As the reaction progressed white powder began precipitating inside the cell. The obtained polymer was washed continuously with fresh CO_2 for 1 hour to remove the stabilizer and any residual monomers or cross-linker since all the reactants are soluble in CO_2 in those conditions.[26,35,36] After venting the CO_2, a white, dry, free flowing powder was collected. Monodisperse and well-defined dry particles with an average diameter of 3.02±0.70 μm and 7.5 mol % of PMAA (from elemental analysis data) were obtained with 92 % yield. The cross-linked microgels were fully insoluble.

An aqueous dispersion of PP9010 (pH ~ 5) was initially prepared at a concentration of 5 mg/mL, which was left equilibrating for 24 hours. LbL sequential deposition of the PE pairs was performed by adding the PP9010 microgels aqueous dispersion to a PE solution to a final concentration of 0.5 mg/mL in microgels and 10 mM in PE (based on the repeating unit). The microgels were left in contact with each PE solution for 30 min in order to ensure equilibrium. Since the microgels were negatively charged the first layer was always a polycation (PDAC, PAH or PLL). For the strong PE pair (PDAC and PSS) the pH was

NIH-PA Author Manuscript

NIH-PA Author Manuscript

NIH-PA Author Manuscript

adjusted to 7.4 by adding NaOH and HCl solutions; whereas for the weak polyelectrolytes the solution pH was adjusted to a value at which the polyelectrolytes were highly ionized: pH 6 for PAH and 9 for PAA; and pH 7.4 for both PLL and PGA. Afterwards the obtained layered microgels were collected by centrifuging the dispersions for 30 min at 4500 × *g*. Microgels were further rinsed in Milli-Q water at the respective pH by at least 3 centrifugation and re-suspension cycles to remove all non-adsorbed PE. All solutions were freshly prepared. For the infrared spectroscopy analysis all samples were lyophilized overnight.

Microgel Characterization

The zeta potential of the microgels was measured at the assembly pH and 24 °C in a ZetaPALS analyzer (Brookhaven Instruments Corp.) as a function of the bilayer number. Each point is the average of ten independent measurements. Particle size distribution for microparticles in a solution can typically be determined using a Coulter Counter, in which the particle sizing correlates directly to the three dimensional volume of the electrolyte solution being displaced by the individual particles. The permeable nature of the PP9010 hydrogel particles allowed the electrolyte solution to diffuse freely, rendering a measured particle size consistently smaller than the actual size determined under an optical microscope (data not shown). Therefore, the microgel size at 24 °C and 37 °C was determined using a Zeiss Axioskop 2 optical microscope at 400 × magnification with temperature control (THMS 600 hot stage, Linkam Scientific Instruments) – the microgel size equilibrated within seconds. Measurements were performed as a function of pH for the uncoated PP9010 microgels and of the layer number for LbL assembled microgels at assembly pH. Each point is the average of at least 100 different microgel particles (qualitatively no significant hysteresis in size was observed when particles were heat cycled from 24 °C to 37 °C and then cooled back to 24 °C).

Fluorescent-labeled polyelectrolyte preparation and analysis

Rhodamine B-labeled PAH (PAHRhodamine B) and cascade blue-labeled PAA (PAA-Cascade Blue) were prepared by modifying the protocols present in the literature,[37,38] and used for the LbL assembly of PP9010 microgels. Briefly, a solution of rhodamine B isothiocyanate in methanol was prepared at 1 mg/mL and added drop-wise to a solution of 2 mg/mL PAH in 0.1 M sodium carbonate buffer at pH 9.0 (2 vol % dye to polymer solutions). The reaction was performed at room temperature under stirring for 6 hours. The dye-conjugated polymer was purified by dialysis (M_W cut-off 10,000) against water until no fluorescence was detected (about 3 days) – the content in rhodamine B was 0.1 mol % per mol of monomer as determined by absorbance measurements. The dialyzed polymer solution was lyophilized. In regards to PAA, 10 equivalents of EDC (1.92 mg, 10 μmol) and HOBt (1.35 mg; 10 mmol) were added to a solution of PAA (120 mg, 1 μmol) in anhydrous DMF (3 mL) and the mixture was stirred under argon for 1 hour. A solution of cascade blue ethylenediamine was prepared separately in anhydrous DMF (3 mL) and added to the reaction. The reaction proceeded for 24 hours. The labeled polymer was purified by dialysis (M_W cut-off 10,000) against Milli-Q water (about 4 days) and lyophilized. The conjugation was assessed by thin layer chromatography using methanol as mobile phase. LbL assembly of dye-labeled polymers was performed as described previously. The microgels were observed when dispersed in PBS on a CARV II spinning disk confocal system equipped with an environmental chamber and a Zeiss inverted microscope. The PP9010 microgels assembled with dye-labeled polyelectrolytes were also analyzed for fluorescence intensity up to 4 bilayers by flow cytometry using aLSR Fortessa HTS (BD Biosciences) and processed using the FlowJo software (Tree Star). Microgels layered with $(PLL\text{-}FITC/PGA)_n$ were excited at 488 nm and monitored at 530/30 nm and those layered with $(PAH\text{-}RhoB/PAA)_n$ were excited at 561 nm and monitored at 610/20 nm. Preliminary gating

NIH-PA Author Manuscript

NIH-PA Author Manuscript

NIH-PA Author Manuscript

isolated events having fluorescence greater than 500 and 2500 for FITC and RhoB labeled microgels respectively. To limit assay interference from debris, the 'autogating tool' (http://www.flowjo.com/v8/html/autogate.html) was applied to select 75–85 % of the remaining events having the most clustered density on a FSC × SSC (forward by side scattering) plot. Reported values are the median fluorescence of this subpopulation.

ATR FT-IR Spectra Analysis

PP9010 microgels, the dry pure polyelectrolytes and the LbL assembled microgels were analyzed by Atenuated Total Reflection Fourier Transform Infrared spectroscopy (ATR FT-IR) in a Thermo Nicolet 6700 FT-IR equipped with a Nicolet Continuum infrared microscope and a MCTA detector. A total of 256 scans were performed with a 4 cm^{-1} resolution and no baseline corrections were performed. The specific interactions in pure PP9010 microgels and between the PP9010 microgels and assembled polyelectrolytes were not always inferred directly from the infrared spectra, because of band overlaps. In order to clarify those interactions, and when necessary, a detailed spectral analysis was made by deconvolution to identify the constituent components of relevant bands, using OriginPro 8.04 software. A non-linear least-squares fitting method was used, assuming Gaussian band profiles for the components. No baseline corrections were made, and no restrictions were imposed on the band positions and widths. The best fits were obtained with reduced $\chi^2 < 10^{-5}$ and a correlation coefficient of ≈ 0.999.

Results and Discussion

LbL assembly on PP9010 microgels

The preparation of microbeads combining pH-responsive PMAA with thermoresponsive PNIPAAm in a copolymer leads to a system sensitive to both pH and temperature. Figure 2a shows the diameter of the microgels, assessed from microscopy, when dispersed in Milli-Q water at different pH (negligible ionic strength) and in buffer solutions at pH 4 and 7.4 with ionic strength adjusted to 160 mM, both at 24 and 37 °C. Overall, the volume of the microgels clearly increases with pH, while the surface charge assessed by zeta potential measurements decreases significantly (Figure 2b). The deprotonation of the PMAA carboxylic groups leads to a Couloumbic repulsion among charged groups and an added osmotic contribution due to mobile counterions migration into the microgel mesh, and a Donnan equilibrium driven swelling occurs.[39] The microgel swelling is lower at higher ionic strength, as the presence of larger concentrations of salt leads to charge shielding of the carboxylate ions. Furthermore, at a pH below the PMAA pK_a (~5–6),[40] the microgels exhibit a clear temperature-dependent swelling behavior, while at values above that pH range the diameter differences at 24 and 37 °C were not significant. This behavior is consistent with turbidimetric analysis at which a clear LCST is observed in a buffer solution at pH 4, while at pH 7.4 no transition is observed upon heating to 50 °C (data not shown). It is well known that the collapse of PNIPAAm-based hydrogels at temperatures above its LCST (~30–32 °C) is an entropy-driven phenomenon in which interactions between PNIPAAm and water become less favorable at higher temperatures. The presence of hydrophilic comonomers has been shown to increase the LCST or even suppress the PNIPAAm intrinsic thermoresponsive behavior, for larger comonomer compositions, by stabilizing the conformation of the polymeric chains in a solvated state.[40] Overall, the striking pH-dependence of the microgel size and zeta potential (Figure 2b) points to a preferential localization of the carboxylic groups on the outer shell of the uncoated microgel, as it has described that ionizable groups located in loosely cross-linked shells enable larger surface charge and swelling degree variations with pH when compared to ionizable groups in the core.[31,41] In addition, poly(NIPAAm-co-MAA) microgels prepared with higher relative amounts of MAA (poly(NIPAAm-co-MAA) 85:15 and 80:20 – data not shown)

NIH-PA Author Manuscript

NIH-PA Author Manuscript

NIH-PA Author Manuscript

under the same conditions in $scCO_2$ had similar zeta potential values across the analyzed pH range, indicating that the PP9010 microgels surface was already saturated with MAA groups (see Supporting Information). Depending on the polymerization conditions, other examples of proposed "core-shell" microstructures in poly(NIPAAm-co-MAA) nanogels are found in the literature.[42,43] A radial distribution of the cross-linker may also contribute to the formation of more dense cores decorated by loosely cross-linked outer shells cross-linked PNIPAAm nanogels.[44]

The LbL assembly of the different PE pairs on PP9010 microgels had an impact on the size and degree of swelling of the microgel (Figure 3). For all the samples dispersed in Milli-Q water at assembly pH, the initial complexation of a polycation leads to a contraction of the microgel, followed by a recovery in size to values close to the native PP9010 microgel upon the subsequent adsorption of the polyanion. In the PP9010/$(PDAC/PSS)_n$ system, the microgels appear to regain and maintain a highly swollen state following the first PSS adsorption step, keeping their size unchanged when measured in the adjusted pH 7.4 conditions of the PE solutions upon further LbL assembly. On the other hand, for both the weak PE pairs the sequential complexation of the polycation leads to microgel contraction for every alternate adsorption step, followed by swelling upon polyanion deposition; this trend is sustained for several assembly cycles. Introduction of buffer solutions at pH 7.4 and 160 mM ionic strength lead to similar oscillations in particle size, but with a much smaller change in gel size due to the shielding of the carboxylic acid groups (see Supporting Information). Moreover, the microgels exhibit a reversible thermoresponsive behavior from 24 °C to 37 °C when a polycation is on the outermost layer of the microgel (except for the PP9010/$(PDAC/PSS)_n$ system after the first bilayer) which is manifest as an increase in size for the 24 °C gel versus 37 °C. The thermoresponsive behavior is suppressed when a polyanion is the last assembled layer (the reversibility of the thermoresponsiveness was qualitatively observed under the microscope as illustrated in Supporting Information). The polycation forms complexes on the PP9010 microgel primarily through ionic interactions with the available carboxylic groups, therefore decreasing the availability of free carboxylate anion groups for swelling and water uptake; as a consequence the microgel swelling decreases, and the entropy-driven collapse of the microgel occurs on increasing temperature, even at pH values above the PMAA pK_a (pH 7.4 for the PP9010/$(PDAC/PSS)_n$ and PP9010/$(PLL/PGA)_n$ and pH 6 for the PP9010/$(PAH/PAA)_n$). The subsequent polyanion complexation occurs via interactions with the underlying polycationic layer at the expense of existing contacts between the polycation and the PP9010 microgel. Therefore, the MAA groups on and within the gel are again freer to stabilize water within the microgel, similar to the native PP9010, and the swelling is recovered while the thermoresponsive behavior is suppressed at pH values above the PMAA pK_a. In addition, the polyanion deposition can also contribute to the higher water content and stabilization of the polyanion-terminated microgels. Contact angle measurements of $(PAH/PSS)_n$ films on rigid planar surfaces have shown that PSS-terminated multilayers are more hydrophilic and thus more swollen.[9] A recent study on the assembly of polypeptides on hyaluronic acid hydrogels has also shown that polyanion-terminated hydrogels were more hydrophilic.[45] However, the subsequent PDAC deposition on the PP9010/$(PDAC/PSS)_n$ microgels did not change the microgel responsiveness significantly. Possibly, the high degree of ionic cross-links formed within the first PDAC/PSS bilayer coupled with the strength of the ionic complexes of the two strong polyelectrolytes, and a lower mobility of the PE chains impairs any effect of further layers on the overall responsiveness of the LbL assembled microgel. The size and thermoresponsive behavior of the microgels is more strongly dependent on the outermost layer (an "odd"/positive or "even"/negative layer)[30] for the PP9010/$(PLL/PGA)_n$ microgels than for the PP9010/$(PAH/PAA)_n$, even though both systems were assembled under conditions where all polyelectrolytes were highly ionized. Previous studies on LbL polypeptide assembly on rigid flat surfaces have shown PE interdiffusion during film build-

NIH-PA Author Manuscript

NIH-PA Author Manuscript

NIH-PA Author Manuscript

up.[19,20] Thus, in soft porous microgels, the polycation/polyanion specific effect on the gel behavior may be more easily reversed in the PLL/PGA than in the PAH/PAA multilayer films. Consistent with the behavior of native PP9010 microgels, when LbL assembled microgels were buffer exchanged to solutions with physiological ionic strength, the presence of salts shields electrostatic repulsions within the microgels and assembled PE pairs, weakening their interactions. For the strong PE system, the presence of salts yielded PDAC-terminated microgels able to respond to temperature stimuli for all bilayer numbers; salt is generally known to decrease, and at high molarity even break up the ionic complexation of strong PE pair LbL films, and thus may enable more direct interaction of these polyelectrolytes with the microgel under buffer conditions. For the weak polyelectrolytes, there were less sharp differences in size and thermoresponsiveness among polycation and polyanion-terminated microgels (Supporting Information). These results are not totally in agreement with other studies performed using poly(NIPAAm-co-MAA) microgels with hydrodynamic radius between ~ 200–360 nm and approximately the same PMAA content and cross-linking degree,[30,33] as in the latter the polyanion terminated microgels retained the thermoresponsive behavior. This disparity may be due to different charge distributions within the microgels, which was shown to impact the thermoresponsive behavior[30] and localization of complexed polyelectrolytes;[31] and/or larger mesh sizes for the microgels used in this study that might allow further interpenetration of the polyelectrolytes contributing to enhance water stabilization within the hydrogel.

Evidence on the sequential deposition of the different polyelectrolytes on PP9010 microgels can be assessed using zeta potential measurements as a function of layer number, at the conditions used during assembly. In Figure 4 it is clear that the surface charge of the microgel was reversed with each assembly step, suggesting that the polyelectrolytes were sequentially complexed. However, in terms of absolute value, the surface charge was not totally reversed upon sequential layering, differing from what is observed for LbL assembly on flat surfaces or rigid particles.[5,8] This behavior is an indication that interactions between the soft and porous microgel substrate and the LbL films are occurring and may be due to incomplete coverage of the microgel surface and/or interpenetration of the polyelectrolytes within the microgel mesh.

Further indications of the successful assembly of the polyelectrolytes is clearly shown in Figure 5 for the PP9010/$(PAH/PAA)_n$ and PP9010/$(PLL/PGA)_n$ systems using fluorescent-labeled polymers, especially for the dual labeled PP9010/$(PAH\text{-Rhodamine B}/PAA\text{-Cascade Blue})_1$ micrograph. Moreover, for both systems, the fluorescent labeling of the polyions has shown that these polyions diffuse into and distribute across the microgel, with higher fluorescence intensity concentrated on the microgel outer shell. This is consistent with the hypothesis that higher concentrations of carboxylic acid groups on the microgel outer shell; another explanation for the higher concentration at the outer shell may be a self-limiting adsorption process that occurs as polycation adsorbs to the top microgel surface even as it diffuses into the gel, thus creating an intrinsic barrier to the diffusion of additional polymer into the gel. The presence of labeled polymer within the gel implies that polyelectrolytes with higher intrinsic mobility may present more significant outermost layer “odd-even” effects based on size and responsive behavior, as increased mobility provides a greater access to the acid groups throughout the microgel, and the ability to titrate those acid groups with subsequent adsorption cycles. On the other hand, it may be argued that the polydispersity of the commercial polyelectrolytes would result in differentiated fluorescence intensity distributions. Further experiments would be required to assess carboxylic groups’ localization within the microgels. The flow cytometry assessment of PP9010/$(PLL\text{-FITC}/PGA)_n$ and PP9010/$(PAH\text{-Rhodamine B}/PAA)_n$ microgels also support the sequential deposition of the polyelectrolytes, showing a successive increase in fluorescence at each polycation deposition step, in an apparently linear regime within the analyzed bilayer

NIH-PA Author Manuscript

NIH-PA Author Manuscript

NIH-PA Author Manuscript

number range. Flow cytometry had already been proposed as a method for monitoring PE assembly on colloidal particles; herein it is shown that it can also be easily expanded for the quick and quantitative evaluation of LbL build-up of multilayers on soft porous particles.[46]

ATR FT-IR spectral analysis of PP9010 and assembled microgels

The assembly of the PE pairs used on PP9010 microgels was further inferred from the sequential modifications in the position, intensity and shape of the infrared bands of the dry assembled microgel FT-IR spectra in the wavenumber region between 950 and 1800 cm^{-1} (see Figure 6). Upon deposition of the first PDAC layer on PP9010, the Amide III band at 1242 cm^{-1} of the PNIPAAm segments became more intense, which was observed as a shoulder in the native microgels (PDAC has no infrared bands around this position – Supporting Information). In addition, the shoulder corresponding to the C=O stretching of unprotonated carboxylic groups of PMAA at 1707 cm^{-1} (besides a small possible contribution of free C=O groups from PNIPAAm) decreased in intensity, indicating that PDAC layering occurs primarily through ionic interactions.[47] The sequential assembly of PSS is indicated by the appearance of the characteristic sulfonate ion vibrations at 1008, 1035, 1126 and 1180 cm^{-1}.[48] These vibrations decrease when PDAC is subsequently assembled (PP9010/$(PDAC/SPS)_1$PDAC spectra), which may be due to interactions being established between the polyelectrolytes [48,49] or partial stripping of the underlying PSS when the polycation was deposited. Nevertheless there was an overall increase of the sulfonate ion bands intensity with bilayer number. The same tendency was observed in the weak PE pairs deposition. However in both systems the most intense and characteristic bands of the polyelectrolytes overlap with the PP9010 amide vibrations (Supporting Information). The exact band positions for the polypeptides depends on their conformation (α-helix, β-sheet or random coil), due to vibrational interactions between the peptide groups and the different forms of hydrogen bonding,[50] while for the weak synthetic polyelectrolytes system, the exact peak positions are related to their degree of ionization.[12,51] For both PE pairs the Amide region becomes less sharp with increasing layer number and it is possible to observe a modification on the peaks position and relative intensity of the Amide II to Amide I bands. Furthermore, in the high wavenumber region of the spectra the sequential deposition of the PLL/PGA and PAH/PAA lead to a relative increase in intensity and broadening of the band in the N-H stretching region between 3000–3450 cm^{-1} relative to the isopropyl and alkyl vibrations (2850–3000 cm^{-1}), due mainly to the contribution of PLL and PAH νN-H and PGA and PAA νO-H (Supporting Information).

From the spectral analysis of the amide region of native and LbL assembled microgels, more information regarding the specific interactions being established can be derived. The spectra of the native PP9010 microgels is dominated by two strong bands at 1641 cm^{-1} and 1531 cm^{-1}, corresponding to the Amide I and Amide II vibrations of the PNIPAAm segments, respectively (with possible contributions of the PMAA carboxylate ion vibration reported at 1554 cm^{-1}).[51,52] Both Amides are slightly shifted to lower energy states in comparison to the amide bands of PNIPAAm homopolymers (1646 and 1533 cm^{-1}, respectively),[26] indicating the formation of hydrogen bonding interactions, similar to what has been reported for the Amide I vibration of other acrylamide copolymers.[53] Upon spectral deconvolution, two components were identified in the Amide I region at 1637 and 1662 cm^{-1}, corresponding to intermolecular and intramolecular H-bonded νC=O vibrations, with the majority involved in intramolecular interactions. In regards to the Amide II vibration, two components were assigned to free δNH vibrations at 1509 cm^{-1} and H-bonded δNH at 1535 cm^{-1} (Table S1, Supporting Information).[52] In both bands, a characteristic component, relative to intermolecular H-bonded νC=O in Amide I and relative to intramolecular H-bonded δNH in Amide II, was absent, which can be an indication of interactions between

NIH-PA Author Manuscript

NIH-PA Author Manuscript

NIH-PA Author Manuscript

NIPAAm amide and MAA carboxylic groups, similarly to what was observed in other systems involving PNIPAAm.[52]

The spectral deconvolution of the LbL assembled microgels in the Amide region (1480–1750 cm^{-1}) enabled further information on the interactions being established between the polyelectrolytes and the underlying PP9010 microbeads. The PP9010/$(PDAC/PSS)_n$ samples can be used as a benchmark for the overall spectral analysis as there are no characteristic bands of the polyelectrolytes overlapping with the PP9010 Amide vibrations. In the PP9010/PDAC system, the constituent bands of the Amide bands shifted significantly to higher energy states, closer to the characteristic vibrations of crosslinked PNIPAAm homopolymers (δNH at 1543 cm^{-1}, intramolecular H-bonded νC=O at 1644 cm^{-1} and "freer" νC=O at 1669 cm^{-1}), pointing that the PNIPAAm segments became "freer" (see Supporting Information). The subsequent adsorption of PSS (PP9010/$(PDAC/PSS)_1$) led to a significant shift of the intramolecular H-bonded νC=O (1632 cm^{-1}) and "freer" νC=O (1653 cm^{-1}) components back to the lower wavenumbers characteristic of the native PP9010, while the intensity of the free νC=O of PMAA COOH group was maintained low, indicating that the PNIPAAm segments were again involved in H-bonding. The deposition of additional strong polyelectrolytes layers did not change the band composition significantly, within the analyzed range. For the weak polyelectrolyte pairs the same tendency was observed in the Amide bands region when the first polycation and subsequently the polyanion were assembled. Moreover, a component assigned to a polyelectrolyte specific vibration occurred at 1615–1630 cm^{-1} which may be due to specific contributions of the polycations.[12,50] However, these systems differ from the strong polyelectrolyte pair as the weak polycation assembly on the first PP9010/$(PAH/PAA)_1$ and PP9010/$(PLL/PGA)_1$ bilayer led again to an Amide bands composition and constituent components intensity similar to the initial PP9010/polycation profile in a quasi-reversible process. The spectral analysis was not performed beyond the second bilayer since the vibrations of the weak polyelectrolytes become predominant over those of the PP9010 substrate. Clearly the spectral analysis correlates well with the observed swelling and thermoresponsive behavior described earlier, suggesting that when polycations are on the outermost layer, PNIPAAm segments are freer to undergo the entropy-driven collapse with increasing temperature, while in polyanion-terminated microgels the water-amide interactions are stabilized. For PP9010/$(PDAC/PSS)_n$ microgels the ionic crosslinking of the first bilayer prevents any further modification of the water-PNIPAAm interactions upon further adsorption cycles.

Conclusions

The LbL sequential deposition of both strong and weak polyelectrolyte pairs on temperature and pH-sensitive poly(NIPAAm-co-MAA) microgels is a complex phenomenon that can be systemically explored to fine tune the microgel native properties and responsive behavior. These microgels were initially prepared by polymerization in supercritical carbon dioxide, rendering monodisperse microparticles that exhibited reversible swelling responses to both temperature and pH. The assembly of polyelectrolytes enables a novel microgel behavior due to an alternating charge distribution within the film that is sensitive to each deposited layer. Overall, polycation-terminated microgels are less swollen and thermoresponsive, even at a pH above the PMAA pK_a; while polyanion-terminated assembled microgels are more swollen and do not exhibit significant volume phase transitions with temperature. The observed "odd-even" layer number effect on microgel swelling and responsiveness is more significant when polyelectrolyte pairs with higher mobility are assembled, PLL/PGA, and is no longer observed for the strong polyelectrolyte pair, PDAC/PSS, after a first highly ionic cross-linked bilayer is established. In addition, increasing the solution ionic strength dampens the multilayer composition influence on the microgel properties. ATR FT-IR

NIH-PA Author Manuscript

NIH-PA Author Manuscript

NIH-PA Author Manuscript

spectral analysis was used as a tool for probing the molecular mechanism of assembly between microgel and polyelectrolytes and the effect on microgel behavior. It was shown that the copolymer carboxylic groups are clearly engaged on the initial complexation of the polycation, which leads to microgel deswelling. Moreover, when a polycation is present as the outermost layer, the NIPAAm segments are “freer” and the microgels become sensitive to temperature stimulus. As a polyanion is assembled, the interaction between the underlying polycation and the microgels weakens and not only NIPAAm segments are again involved in H-bonding interactions but also carboxylic groups can deprotonate leading to microgel swelling. Potentially, the polyanions hydrophilic character can also contribute to the stabilization of the microgel in a solvated state.

This study clearly shows that complexation of macromolecules on stimuli-responsive systems may significantly impact their properties. But more importantly, it can be used to modify these systems for specific applications in which environmentally triggered changes in surface chemistry, size, water content or net charge may be explored, such as biosensing and macromolecules loading or controlled release.

Supplementary Material

Refer to Web version on PubMed Central for supplementary material.

Acknowledgments

This project was funded in part by the MIT-Portugal Program (Bioengineering Systems Focus Area). The authors thank the financial support from the Fundação para a Ciência e Tecnologia (FCT) through the doctoral grant SFRH / BD / 35382 / 2007 (E.C.), project MIT-Pt/BSCTRM/ 0051/2008, FEDER, FSE and POCTI, and from the National Institutes of Health (NIH).

References

1. Decher G. Fuzzy Nanoassemblies: Toward Layered Polymeric Multicomposites. Science. 1997; 277:1232–1237.
2. Stubbe BG, Gevaert K, Derveaux S, Braeckmans K, De Geest BG, Goethals M, Vandekerckhove J, Demeester J, De Smedt SC. Evaluation of Encoded Layer-By-Layer Coated Microparticles as Protease Sensors. Adv Funct Mater. 2008; 18:1624–1631.
3. Stubbe BG, Gevaert K, Derveaux S, Braeckmans K, De Geest BG, Goethals M, Vandekerckhove J, Demeester J, De Smedt SC. Evaluation of Encoded Layer-By-Layer Coated Microparticles as Protease Sensors. Adv Funct Mater. 2008; 18:1624–1631.
4. Cortez C, Tomaskovic-Crook E, Johnston APR, Radt B, Cody SH, Scott AM, Nice EC, Heath JK, Caruso F. Targeting and Uptake of Multilayered Particles to Colorectal Cancer Cells. Adv Mater. 2006; 18:1998–2003.
5. Rogach A, Susha A, Caruso F, Sukhorukov G, Kornowski A, Kershaw S, Möhwald H, Eychmüller A, Weller H. Nano- and Microengineering: 3-D Colloidal Photonic Crystals Prepared from Sub-μm-sized Polystyrene Latex Spheres Pre-Coated with Luminescent Polyelectrolyte/Nanocrystal Shells. Adv Mater. 2000; 12:333–337.
6. Peyratout CS, Dähne L. Tailor-made polyelectrolyte microcapsules: from multilayers to smart containers. Angew Chem, Int Ed. 2004; 43:3762–3783.
7. Hammond PT. Form and Function in Multilayer Assembly: New Applications at the Nanoscale. Adv Mater. 2004; 16:1271–1293.
8. Itano K, Choi J, Rubner MF. Mechanism of the pH-Induced Discontinuous Swelling / Deswelling Transitions of Poly (allylamine hydrochloride)-Containing Polyelectrolyte Multilayer Films. Macromolecules. 2005; 38:3450–3460.
9. Wong JE, Rehfeldt F, Hänni P, Tanaka M, Klitzing RV. Swelling Behavior of Polyelectrolyte Multilayers in Saturated Water Vapor. Macromolecules. 2004; 37:7285–7289.

NIH-PA Author Manuscript

NIH-PA Author Manuscript

NIH-PA Author Manuscript

10. Farhat TR, Schlenoff JB. Doping-controlled ion diffusion in polyelectrolyte multilayers: mass transport in reluctant exchangers. J Am Chem Soc. 2003; 125:4627–36. [PubMed: 12683835]
11. Farhat T, Yassin G, Dubas ST, Schlenoff JB. Water and Ion Pairing in Polyelectrolyte Multilayers. Langmuir. 1999; 15:6621–6623.
12. Choi J, Rubner MF. Influence of the Degree of Ionization on Weak Polyelectrolyte Multilayer Assembly. Macromolecules. 2005; 38:116–124.
13. Mendelsohn JD, Yang SY, Hiller J, Hochbaum AI, Rubner MF. Rational Design of Cytophilic and Cytophobic Polyelectrolyte Multilayer Thin Films. Biomacromolecules. 2003; 4:96–106. [PubMed: 12523853]
14. Hiller J, Mendelsohn JD, Rubner MF. Reversibly Erasable Nanoporous Anti-Reflection Coatings from Polyelectrolyte Multilayers. Nat Mater. 2002; 1:59–63. [PubMed: 12618851]
15. Chia KK, Cohen RE, Rubner MF. Amine-Rich Polyelectrolyte Multilayer Nanoreactors for in Situ Gold Nanoparticle Synthesis. Chem Mater. 2008; 20:6756–6763.
16. Richert L, Lavalle P, Vautier D, Senger B, Stoltz JF, Schaaf P, Voegel JC, Picart C. Cell Interactions with Polyelectrolyte Multilayer Films. Biomacromolecules. 2002; 3:1170–1178. [PubMed: 12425653]
17. Serizawa T, Yamaguchi M, Akashi M. Alternating Bioactivity of Polymeric Layer-by-Layer Assemblies: Anticoagulation Vs Procoagulation of Human Blood. Biomacromolecules. 2002; 3:724–731. [PubMed: 12099816]
18. Richert L, Boulmedais F, Lavalle P, Mutterer J, Ferreux E, Decher G, Schaaf P, Voegel JC, Picart C. Improvement of Stability and Cell Adhesion Properties of Polyelectrolyte Multilayer Films by Chemical Cross-Linking. Biomacromolecules. 2004; 5:284–294. [PubMed: 15002986]
19. Picart C. Polyelectrolyte Multilayer Films: from Physico-Chemical Properties to the Control of Cellular Processes. Curr Med Chem. 2008; 15:685–697. [PubMed: 18336282]
20. Jourdainne L, Lecuyer S, Arntz Y, Picart C, Schaaf P, Senger B, Voegel JC, Lavalle P, Charitat T. Dynamics of Poly(L-lysine) in Hyaluronic Acid/Poly(L-lysine) Multilayer Films Studied by Fluorescence Recovery after Pattern Photobleaching. Langmuir. 2008; 24:7842–7847. [PubMed: 18582004]
21. Nayak S, Lyon LA. Soft Nanotechnology with Soft Nanoparticles. Angew Chem, Int Ed. 2005; 44:7686–7708.
22. Heskins M, Guillet JE. Solution Properties of Poly (*N*-isopropylacrylamide). J Macromol Sci Chem. 1968; 2:37–41.
23. Schild HG. Poly(*N*-isopropylacrylamide) - Experiment, Theory and Application. Prog Polym Sci. 1992; 17:163–249.
24. Hoare T, Pelton R. Highly pH and Temperature Responsive Microgels Functionalized with Vinylacetic Acid. Macromolecules. 2004; 37:2544–2550.
25. Temtem M, Casimiro T, Mano JF, Aguiar-Ricardo A. Green Synthesis of a Temperature Sensitive Hydrogel. Green Chem. 2007; 9:75–79.
26. Costa E, de-Carvalho J, Casimiro T, Lobato da Silva C, Cidade MT, Aguiar-Ricardo A. Tailoring Thermoresponsive Microbeads in Supercritical Carbon Dioxide for Biomedical Applications. J Supercrit Fluid. 2011; 56:292–298.
27. Shenoy DB, Antipov AA, Sukhorukov GB, Möhwald H. Layer-by-Layer Engineering of Biocompatible, Decomposable Core-Shell Structures. Biomacromolecules. 2003; 4:265–272. [PubMed: 12625721]
28. Ochs C, Such G, Stadler B, Caruso F. Low-Fouling, Biofunctionalized, and Biodegradable Click Capsules. Biomacromolecules. 2008; 9:3389–3396. [PubMed: 18991459]
29. De Geest BG, De Koker S, Demeester J, De Smedt SC, Hennink WE. Pulsed In Vitro Release and In Vivo Behavior of Exploding Microcapsules. J Control Release. 2009; 135:268–273. [PubMed: 19331854]
30. Wong JE, Richtering W. Surface Modification of Thermoresponsive Microgels via Layer-by-Layer Assembly of Polyelectrolyte Multilayers. Prog Coll Pol Sci. 2006; 133:45–51.
31. Kleinen J, Klee A, Richtering W. Influence of Architecture on the Interaction of Negatively Charged Multisensitive Poly(*N*-Isopropylacrylamide)-co-Methacrylic Acid Microgels with

NIH-PA Author Manuscript

NIH-PA Author Manuscript

NIH-PA Author Manuscript

Oppositely Charged Polyelectrolyte: Absorption Vs Adsorption. Langmuir. 2010; 26:11258–11265. [PubMed: 20377221]

32. Wong JE, Díez-Pascual AM, Richtering W. Layer-by-Layer Assembly of Polyelectrolyte Multilayers on Thermoresponsive P(NiPAM-co-MAA) Microgel: Effect of Ionic Strength and Molecular Weight. Macromolecules. 2009; 42:1229–1238.
33. Díez-Pascual AM, Wong JE. Effect of Layer-by-Layer Confinement of Polypeptides and Polysaccharides onto Thermoresponsive Microgels: a Comparative Study. J Colloid Interf Sci. 2010; 347:79–89.
34. Casimiro T, Banet-Osuna AM, Ramos AM, da Ponte MN, Aguiar-Ricardo A. Synthesis of Highly Cross-Linked Poly(Diethylene Glycol Dimethacrylate) Microparticles in Supercritical Carbon Dioxide. Eur Polym J. 2005; 41:1947–1953.
35. Christian P, Howdle SM, Irvine DJ. Dispersion Polymerization of Methyl Methacrylate in Supercritical Carbon Dioxide with a Monofunctional Pseudo-Graft Stabilizer. Macromolecules. 2000; 33:237–239.
36. Casimiro T, Shariati A, Peters CJ, da Ponte MN, Aguiar-Ricardo A. Phase Behavior Studies of a Perfluoropolyether in High-Pressure Carbon Dioxide. Fluid Phase Equilibr. 2004; 224:257–261.
37. Ibarz G, Dähne L, Donath E, Möhwald H. Smart Micro- and Nanocontainers for Storage, Transport, and Release. Adv Mater. 2001; 13:1324–1327.
38. Christian DA, Tian A, Ellenbroek WG, Levental I, Rajagopal K, Janmey PA, Liu AJ, Baumgart T, Discher DE. Spotted Vesicles, Striped Micelles and Janus Assemblies Induced by Ligand Binding. Nat Mater. 2009; 8:843–849. [PubMed: 19734886]
39. Flory, PJ. Principles of Polymer Chemistry. Cornell Un; London: 1986.
40. Brazel CS, Peppas NA. Synthesis and Characterization of Thermo- and Chemomechanically Responsive Poly(N-isopropylacrylamide-co-methacrylic acid) Hydrogels. Macromolecules. 1995; 28:8016–8020.
41. Jones CD, Lyon LA. Shell-Restricted Swelling and Core Compression in Poly(N -isopropylacrylamide) Core–Shell Microgels. Macromolecules. 2003; 36:1988–1993.
42. Hoare T, Pelton R. Functional Group Distributions in Carboxylic Acid Containing poly(*N*-Isopropylacrylamide) Microgels. Langmuir. 2004; 20:2123–2133. [PubMed: 15835661]
43. Zhou S, Chu B. Synthesis and Volume Phase Transition of Poly(methacrylic acid-co-N-Isopropylacrylamide) Microgel Particles in Water. J Phys Chem B. 1998; 102:1364–1371.
44. Varga I, Gilányi T, Mészáros R, Filipcsei G, Zrínyi M. Effect of Cross-Link Density on the Internal Structure of Poly(*N*-isopropylacrylamide) Microgels. J Phys Chem B. 2001; 105:9071–9076.
45. Yamanlar S, Sant S, Boudou T, Picart C, Khademhosseini A. Surface functionalization of hyaluronic acid hydrogels by polyelectrolyte multilayer films. Biomaterials. 2011; 32:5590–5599. [PubMed: 21571364]
46. Johnston APR, Zelikin AN, Lee L, Caruso F. Approaches to Quantifying and Visualizing Polyelectrolyte Multilayer Film Formation on Particles. Anal Chem. 2006; 78:5913–5919. [PubMed: 16906740]
47. Garcia D, Escobar J, Bada N, Casquero J, Hernaez E, Katime I. Synthesis and Characterization of Poly(Methacrylic Acid) Hydrogels for Metoclopramide Delivery. Eur Polym J. 2004; 40:1637–1643.
48. Fan XD, Bazuin CG. Sulfonated Polystyrene Ionomers Neutralized by Bi- and Multifunctional Organic Cations. 1. An Infrared Spectroscopic Study. Macromolecules. 1995; 28:8209–8215.
49. Gregoriou VG, Hapanowicz R, Clark SL, Hammond PT. Infrared Studies of Novel Optically Responsive Materials: Orientation Characteristics of Sulfonated Polystyrene/Poly(diallyldimethylammonium Chloride) Ionic Polymer Multilayers on Patterned Self-Assembled Monolayers. Appl Spectrosc. 1997; 51:470–476.
50. Lee NH, Frank CW. Surface-Initiated Vapor Polymerization of Various α-Amino Acids. Langmuir. 2003; 19:1295–1303.
51. Sukhishvili SA, Granick S. Erasable Polymer Multilayers Formed by Hydrogen-Bonded Sequential Self-Assembly. Macromolecules. 2002; 35:301–310.

NIH-PA Author Manuscript

NIH-PA Author Manuscript

NIH-PA Author Manuscript

52. Costa E, Coelho M, Ilharco LM, Aguiar-Ricardo A, Hammond PT. Tannic Acid Mediated Suppression of PNIPAAm Microgels Thermoresponsive Behavior. Macromolecules. 2011; 44:612–621.

53. Shibanuma T, Aoki T, Sanui K, Ogata N, Kikuchi A, Sakurai Y, Okano T. Thermosensitive Phase-Separation Behavior of Poly (Acrylic Acid)-graft-Poly (N, N-Dimethylacrylamide) Aqueous Solution. Macromolecules. 2000; 33:444–450.

NIH-PA Author Manuscript

NIH-PA Author Manuscript

NIH-PA Author Manuscript

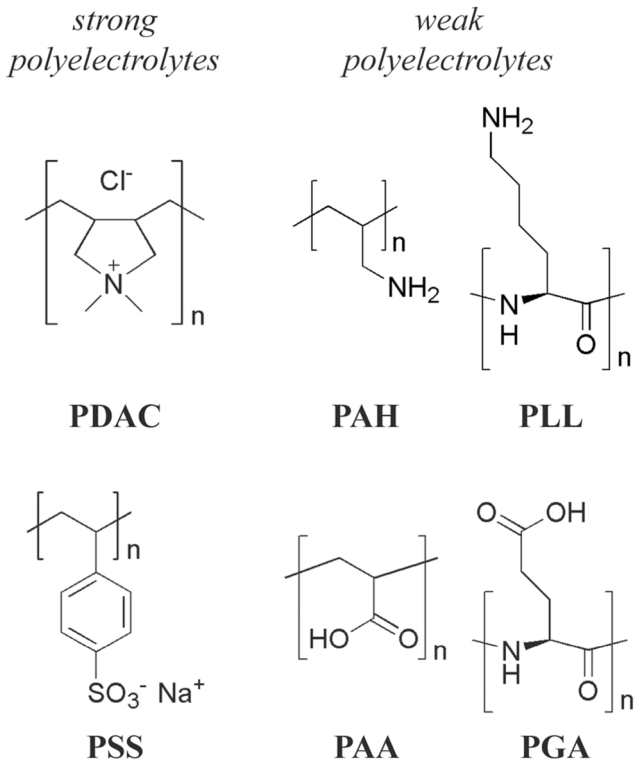

Figure 1.
Chemical structure of the PE pairs assembled on poly(NIPAAm-co-MAA) microgels: poly(diallyldimethylammonium chloride), PDAC, and poly(sodium styrene sulfonate), PSS; poly(allylamine hydrochloride), PAH, and poly(acrylic acid), PAA; poly(L-lysine), PLL, and poly(L-glutamic acid), PGA.

NIH-PA Author Manuscript

NIH-PA Author Manuscript

NIH-PA Author Manuscript

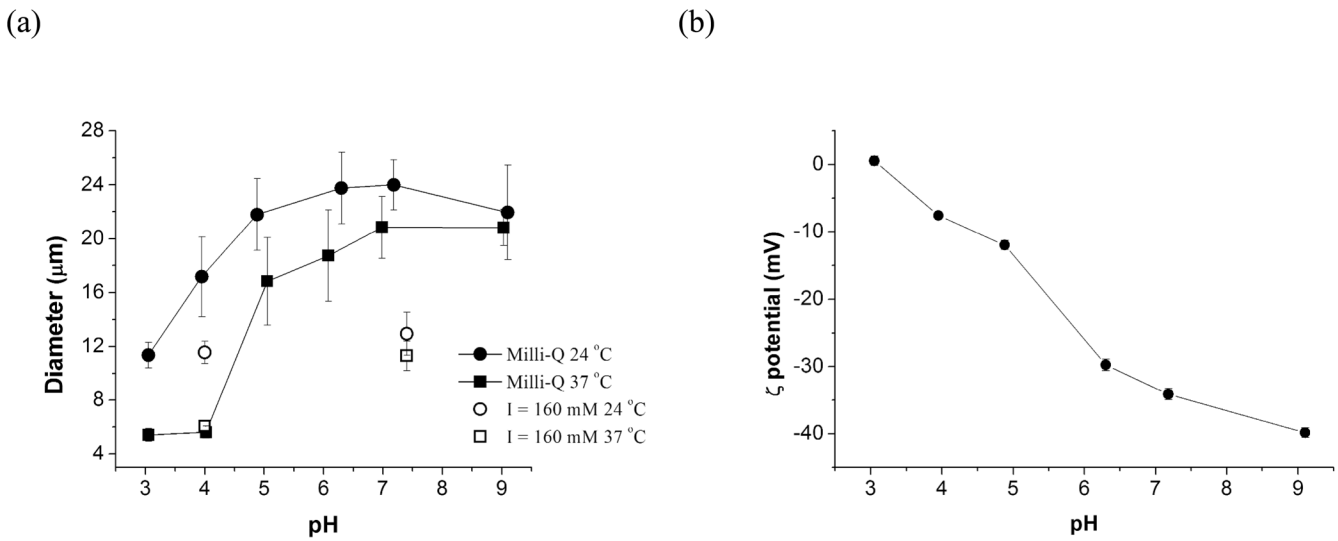

Figure 2.

(a) PP9010 microgel diameter (mean value ± standard deviation) as a function of pH and ionic strength at 24 °C (circles) and 37 °C (squares); closed symbols stand for microgels dispersed in Milli-Q water and open symbols in buffer solutions (I = 160 mM). (b) Zeta potential of PP9010 microgels as a function of pH at 24 °C.

NIH-PA Author Manuscript

NIH-PA Author Manuscript

NIH-PA Author Manuscript

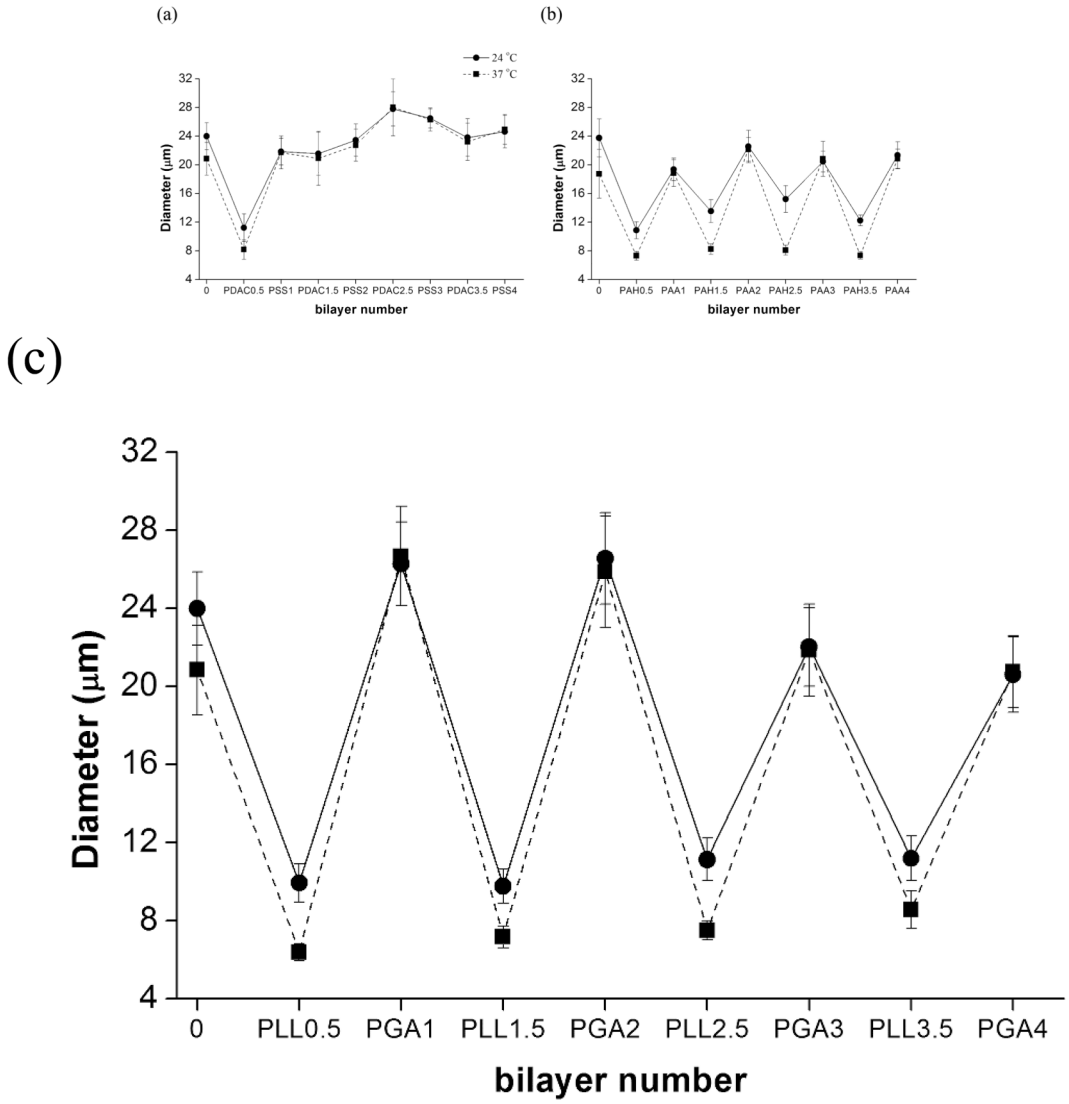

Figure 3.
Particle diameter upon polyelectrolyte LbL on PP9010 microgels in Milli-Q water at the assembly pH and at 24 °C (circles) and 37 °C (squares): (a) PP9010/$(PDAC/PSS)_n$; (b) PP9010/$(PAH/PAA)_n$; and (c) PP9010/$(PLL/PGA)_n$.

NIH-PA Author Manuscript

NIH-PA Author Manuscript

NIH-PA Author Manuscript

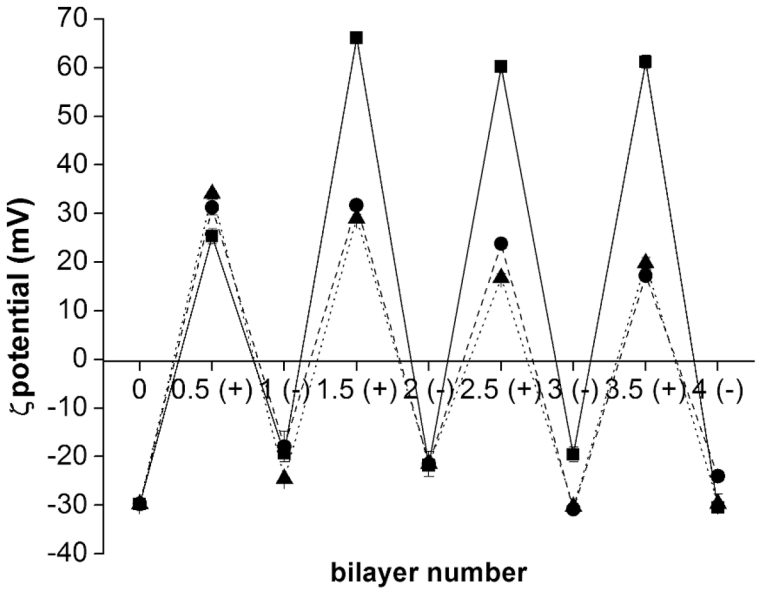

Figure 4.

Zeta potential measurements of LbL assembled microgels with increasing bilayer number showed surface charge reversal upon polyelectrolyte sequential deposition: PP9010/(PDAC/PSS)$_n$ (squares); PP9010/(PAH/PAA)$_n$ (triangles) and PP9010/(PLL/PGA)$_n$ (circles). The initial point (0) refers to the zeta potential of native PP9010 microgels when dispersed in water (pH ~ 5).

NIH-PA Author Manuscript

NIH-PA Author Manuscript

NIH-PA Author Manuscript

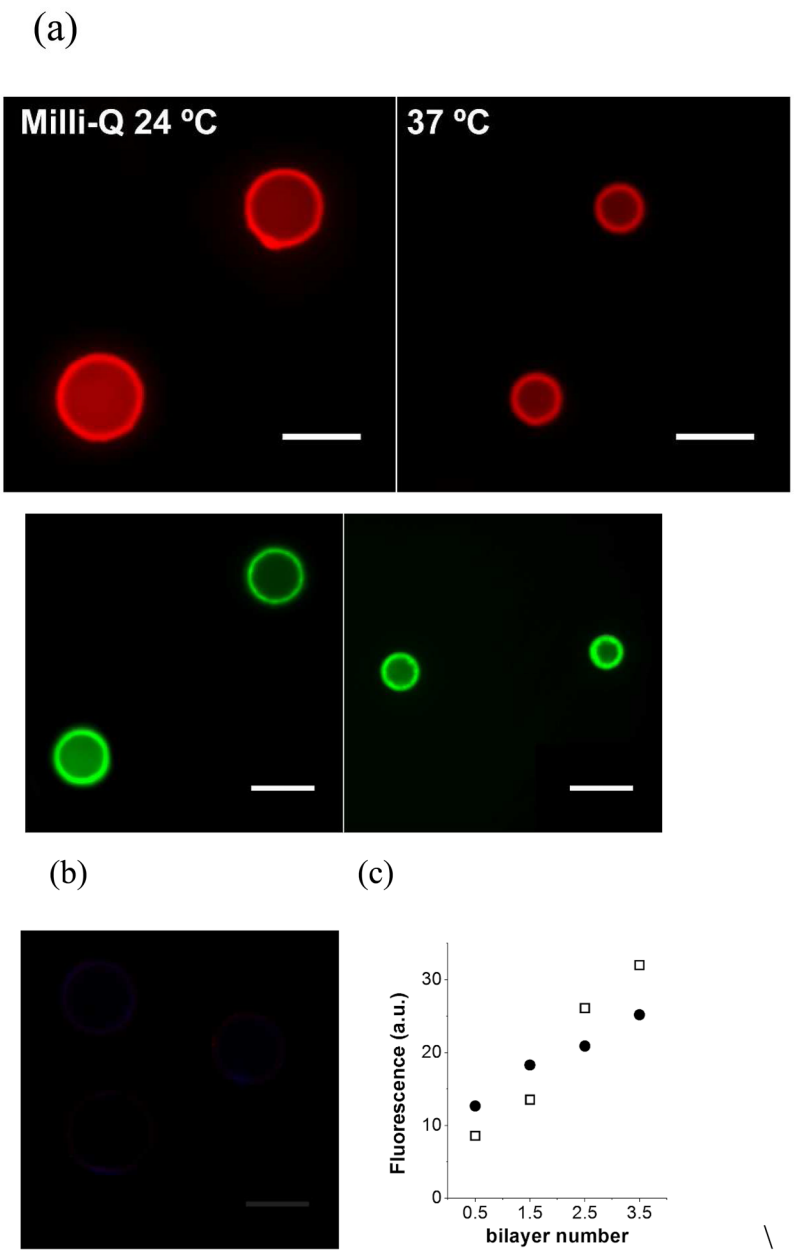

Figure 5.

Fluorescently-labeled polyelectrolytes allowed visualization of multilayers localization by confocal microscopy and quantitative assessment of LbL film growth on PP9010 microgels by flow cytometry: (a) confocal micrographs of PP9010/PAH-Rhodamine B (top) and PP9010/PLL-FITC (bottom) assembled microgels dispersed in Milli-Q water at assembly pH at 24 °C and 37 °C; (b) confocal micrographs of PP9010/(PAH-Rhodamine B/PAA-Cascade Blue)$_1$ indicating multilayer build-up. Scale = 10 μm; and (c) flow cytometry measurements of the fluorescence of PP9010/(PLL-FITC/ PGA)$_n$ (circles) and PP9010/(PAH-RhoB/PAA)$_n$ (open squares) microgels in 10 mM PBS buffer, showing an overall increase in the amount of polycation with bilayer number.

NIH-PA Author Manuscript

NIH-PA Author Manuscript

NIH-PA Author Manuscript

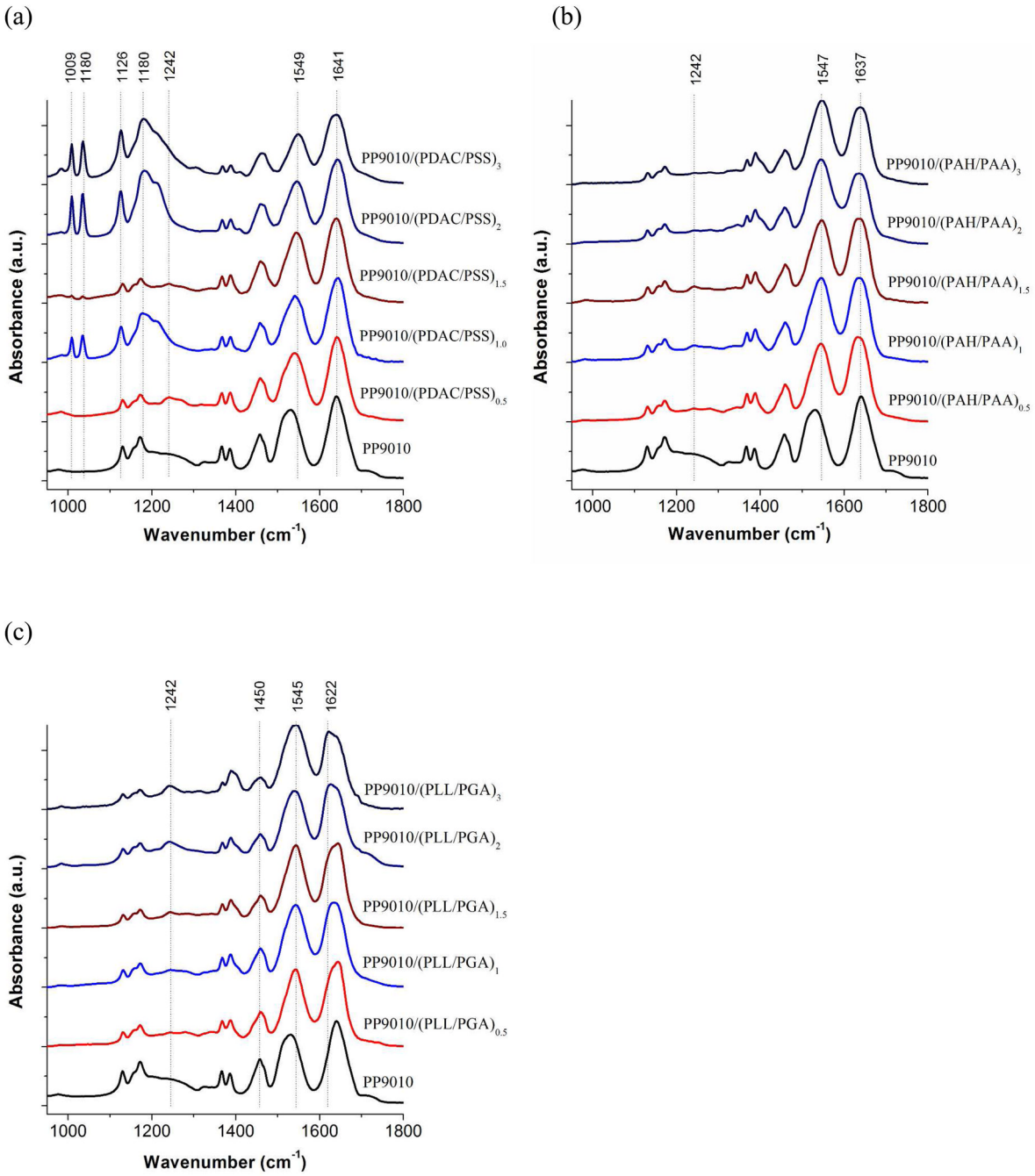

Figure 6.

ATR FT-IR spectra of LbL assembled PP9010 microgels show increase in the absorbance of characteristic components of the polyelectrolytes with the sequential deposition for 0.5, 1, 1.5, 2 and 3 bilayers: (a) PP9010/$(PDAC/PSS)_n$; (b) PP9010/$(PAH/PAA)_n$; (c) PP9010/$(PLL/PGA)_n$.